Journal of Rock Mechanics and Geotechnical Engineering. 2010, 2 (2): 124–128

Journal of Rock Mechanics and Geotechnical Engineering

Journal online: www.rockgeotech.org

Heating pulse tests under constant volume on Boom clay

A. Lima[1], E. Romero[1*], A. Gens[1], J. Muñoz[2], X. L. Li[3]

[1] *Department of Geotechnical Engineering and Geosciences, Universitat Politècnica de Catalunya, Barcelona, Spain*

[2] *Department of Civil Engineering, Universidad Nacional de San Juan, San Juan, Argentina*

[3] *EIG EURIDICE/SCK•CEN, Mol, Belgium*

Received 15 May 2009; received in revised form 14 November 2009; accepted 6 January 2010

Abstract: Boom clay formation is a potential natural host rock for geological disposal of high-level nuclear waste in Belgium. Heating pulse tests with controlled power supply (maximum temperature was limited to 85 °C) and controlled hydraulic boundary conditions were performed under nearly constant volume conditions to study the impact of thermal loading on the clay formation. Selected test results of intact borehole samples retrieved in horizontal direction are presented and discussed. The study focuses on the time evolution of temperature and pore water pressure changes along heating and cooling paths, i.e. pore pressure build-up during quasi-undrained heating and later dissipation at constant temperature.

Key words: natural Boom clay; heating pulse test; pore pressure build-up; pore pressure dissipation

1 Introduction

Boom clay is the subject of extensive research in Belgium dealing with all phenomena that possibly affect the performance of the clay as a potential geological host formation for high-level nuclear waste during gallery construction and final operation. Specifically, thermal loading may play an important role in this low permeability clay. There were a number of laboratory results concerning the saturated hydro-mechanical behaviour of Boom clay under a constant temperature field, and studies in this area were described by Sultan et al. [1–3]. Nevertheless, information on hydro-mechanical response of clay along heating and cooling paths under small-scale laboratory conditions is very limited. Therefore, the paper explores the consequences of thermal loading by presenting selected results of a comprehensive test programme performed on an axi-symmetric heating cell described by Muñoz et al. [4]. The cell was improved in this work to achieve higher temperatures.

Doi: 10.3724/SP.J.1235.2010.00124
*Corresponding author. Tel: +34-93-4016888;
E-mail: enrique.romero-morales@upc.edu
Supported by EIG EURIDICE/SCK• CEN

Heating pulse tests (the maximum temperature was limited to 85 °C) on borehole samples retrieved in the horizontal direction were performed under nearly constant volume and controlled hydraulic boundary conditions, i.e. constant water pressure at the bottom drainage and top end without water flow. Selected testing results are presented and discussed in terms of the joint measurements of temperature and pore water pressure changes at selected points within the sample and along different heating and cooling paths.

2 Experimental programme

2.1 Tested material

Laboratory tests were performed on Boom clay (Mol, Belgium). Table 1 [5] summarises the basic characteristics and the main volumetric and gravimetric properties of this slightly overconsolidated Tertiary clay, which contains 20%–30% kaolinite, 20%–30% illite and 10%–20% smectite [6–8].

A soil sample was trimmed from a borehole sample retrieved in horizontal direction with dimensions of 75 mm in diameter and 100 mm in height (bedding planes are parallel to the direction of axial symmetry). In

Table 1 Main properties of Boom clay [5].

Density, ρ (Mg/m^3)	Dry density, ρ_d (Mg/m^3)	Gravimetric water content, w (%)	Initial total suction, ψ (MPa)	Density of soil solids, ρ_s (Mg/m^3)	Void ratio, e	Porosity, n
1.99–2.05	1.65–1.71	21–25	2–4	2.67	0.560–0.618	0.358–0.382

Degree of saturation, S_r (%)	Liquid limit (using SBCW), w_L (%)	Plasticity index, I_P (%)	Vertical water permeability (T = 20 ºC), k_{wv} (m/s)	Vertical water permeability (T=80 ºC), k_{wv} (m/s)	Horizontal water permeability (T=20 ºC), k_{wh} (m/s)
91–100	56	27	$(2.4–3.1)\times10^{-12}$	6.5×10^{-12}	$(5.7–7.4)\times10^{-12}$

the initial state of the saturated sample, the water content w is 23.2% and the dry density ρ_d is 1.65 Mg/m^3. The water used in the tests was synthetic Boom clay water (SBCW), which has similar composition to the natural water of Boom clay formation.

2.2 Laboratory equipment and tests performed

Figure 1 shows a modified scheme of the axisymmetric heating cell described by Muñoz et al. [4]. A power-controlled heater ("H" in Fig.1) was installed along the axis of the sample in the lower part of the cell. Different transducers were used to monitor the sample response: two miniature pore water pressure transducers, three K-type thermocouples and top and lateral strain gauges attached to thickness-reduced sections. Moreover, the cell had top and bottom valves (u_u and u_b) to apply the hydraulic conditions. The transducers were described by Muñoz et al. [4]. The cell was updated to perform heating paths at temperatures higher than 50 ºC. A data acquisition software was specifically written to log the different transducers.

The main objective is to measure pore water pressure and temperature evolution of the soil during different hydration and heating/cooling paths. The tests have three important phases: hydration, heating and cooling. During the hydration phase, the backpressure (u_b in Fig.1) was increased in steps (0.1 MPa for 3 days, 0.5 MPa for 2 days and 1 MPa for final testing). The upper valve was maintained open under atmospheric conditions during this initial phase. Throughout the course of the heating phase, the bottom drainage was maintained open at a water backpressure of 1 MPa using an automatic pressure/volume controller, while the upper valve was kept closed. This backpressure is important since it allows measuring the pore pressure drop during the cooling phase without invading the negative range (below atmospheric conditions). The initial and external temperatures were always regulated by submerging the cell inside a temperature controlled water bath at 19 ºC.

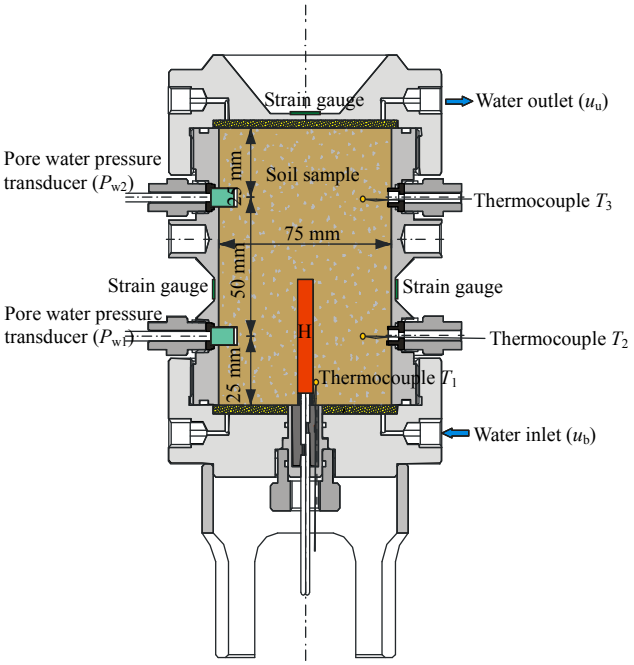

Fig.1 Modified scheme of the heating cell.

The heater with controlled power supply remained switched on for 24 hours during the heating stage and later switched off to perform the cooling phase. Electric power supplied to the heater is shown in Table 2 for different heating stages performed (thermal stages 2–4). Tests ended when soil temperature reached the initial value (around 19 ºC).

Table 2 Testing results in different stages.

Stage	Power supply, P (W)	Max./min. temperature, T_1 (ºC)	P_{w1} (MPa)		P_{w2} (MPa)	
			Heating	Cooling	Heating	Cooling
2	2.78	28/19	1.15	0.81	1.13	0.85
3	9.63	53/19	1.38	0.48	1.39	0.48
4	19.0	85/19	1.69	0.17	1.83	0.13

3 Experimental results

3.1 Hydration phase

Permeability was measured under steady-state conditions during the hydration phase, which was equal to 5.7×10^{-12} m/s and was in agreement with the

horizontal permeability reported in Table 1 (bedding planes are parallel to the direction of axial symmetry). Figure 2(a) shows the time evolution of water outlet volume measured under steady-state condition at backpressure of 1 MPa which was used for the water permeability determination. Figure 2(b) presents the pore water pressure under steady-state conditions with 1 MPa backpressure at different elevations on the sample (0.75 MPa at 25 mm from the bottom, 0.26 MPa at 75 mm and atmospheric conditions at 100 mm). The results adequately confirm the linear relationship of the pressure transducers in this homogeneous soil prior to the thermal phases.

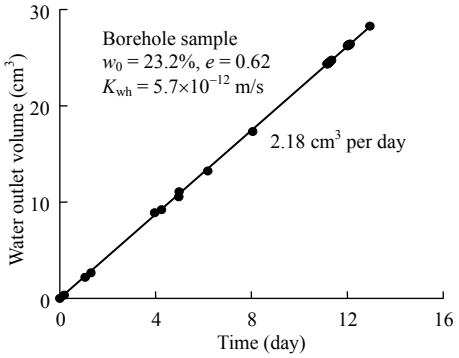

(a) Time evolution of water outlet volume under steady-state condition.

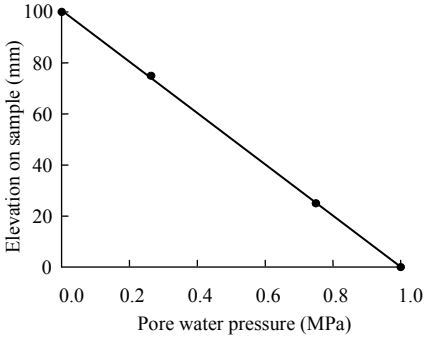

(b) Pore water pressures at different elevations under steady-state condition.

Fig.2 Results of hydration phase.

3.2 Heating and cooling phases

Figures 3–5 show the results obtained in thermal stages 2–4, respectively. The maximum temperature in the heater reached 85 ºC during thermal stage 4 (Fig.5(a)), which was accompanied with a maximum pressure build-up during quasi-undrained heating of 1.83 MPa (P_{w2}), and slightly less than the value at lower pore water pressure transducer (P_{w1}=1.69 MPa), which is placed near the bottom draining boundary (Fig.5(b)). During quasi-undrained cooling and returning to the initial temperature along thermal stage 4, the pore water pressures dropped to 0.13 MPa (P_{w2}) and to 0.17 MPa (P_{w1}), respectively.

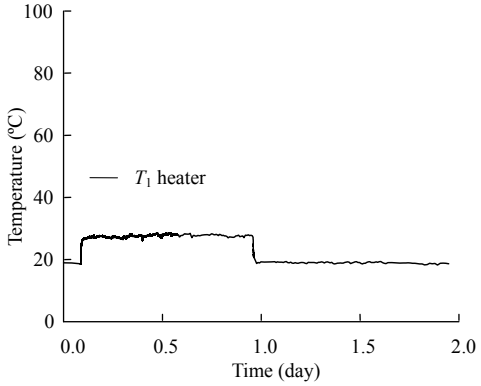

(a) Time evolution of temperature.

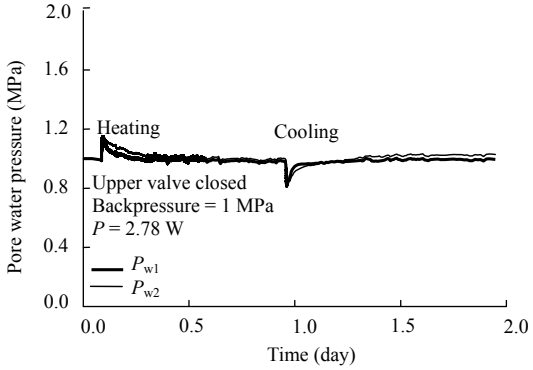

(b) Time evolution of pore water pressure.

Fig.3 Results of thermal stage 2.

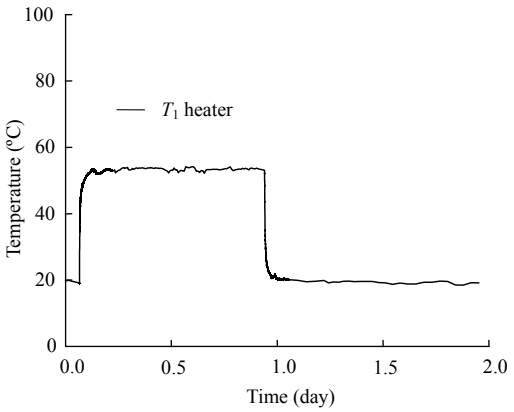

(a) Time evolution of temperature.

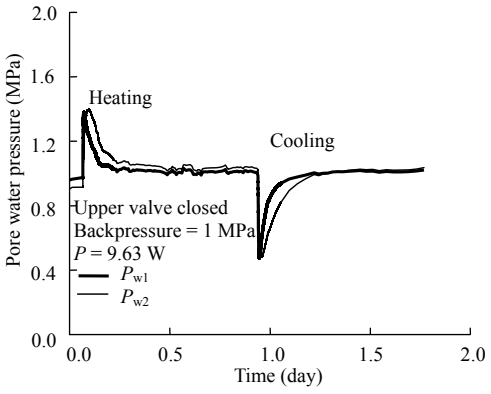

(b) Time evolution of pore water pressure.

Fig.4 Results of thermal stage 3.

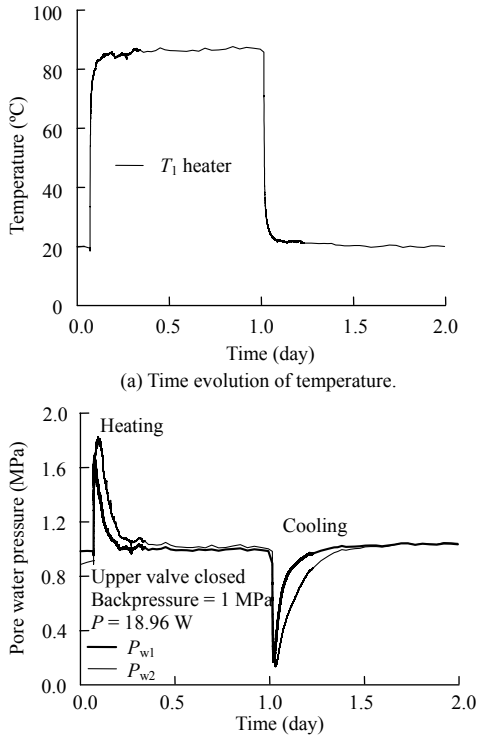

(a) Time evolution of temperature.

(b) Time evolution of pore water pressure.

Fig.5 Results of thermal stage 4.

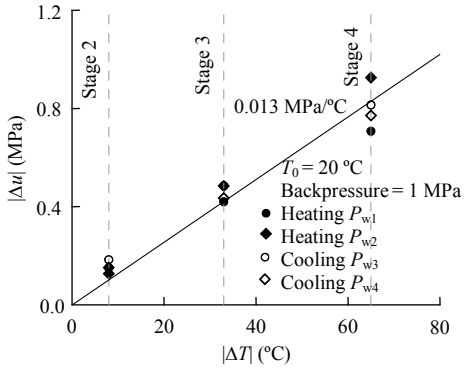

Fig.6 Pore water pressure changes vs. temperature changes at T_1 heater.

Table 2 summarizes the increased maximum temperatures and the corresponding minimum ones by cooling, as well as the pore water pressures obtained from different quasi-undrained heating/cooling stages at the maximum and minimum temperatures.

During heating stage, the pore water pressure increased due to its large thermal expansion coefficient. The changing magnitude of pore water pressure depends on the rate and the range of temperature increase/decrease (quasi-undrained heating), soil compressibility (dependent on the stress state), thermal-expansion coefficient, water permeability, porosity, as well as the applied hydraulic boundary conditions. The change in pore water pressure under thermal loading and saturated conditions was analyzed assuming the volumetric compatibility between soil matrix and their constituents (liquid and solid) using compressibility and thermal expansion coefficients [9, 10]. Figure 6 summarizes the absolute values of the changes in pore water pressure for each thermal stage at maximum/minimum temperatures during quasi-undrained heating/cooling (absolute values of temperature changes are obtained from measuring point T_1 heater). In thermal stage 4, a larger pressure build-up is detected at the upper pore water pressure transducer due to the fact that the measuring point is located at a larger distance from the draining boundary. As observed in Fig.6, the quasi-undrained pressurisation coefficient, defined as the pore pressure increase due to unit temperature increase, around 0.013 MPa/°C is obtained.

As observed in Figs.3(b), 4(b) and 5(b), after the quasi-undrained heating pulse, pore water pressures dissipate at constant temperature towards the value applied by the hydraulic boundary condition (1 MPa). Pore water pressure P_{w2} dissipates more slowly due to its larger distance from the draining bottom boundary. It can be observed in the figures that the time required to dissipate pore water pressure at upper transducer is less than 12 hours. An equivalent phenomenon is observed in these figures after the quasi-undrained cooling, in which pore water pressures increase at constant temperature towards 1 MPa after the initial drop. Again, pore water pressure P_{w2} dissipates more slowly due to its larger distance from the draining bottom boundary.

Figure 7 presents a zoom of the time evolution of pore water pressure (P_{w1}) and temperature (T_2) changes during thermal stage 4 in both heating and cooling phases. These sensors are located close to the draining boundary and at the same height (Fig.1). As observed, changes in water pressure develop at a faster velocity compared with temperature changes during quasi-undrained heating/cooling conditions. In fact, pressures start to dissipate or increase towards the hydraulic boundary condition applied before the temperature reaches its maximum or minimum value in the heating or cooling phase. A similar fast water pressure response compared with temperature was observed when heating under water undrained conditions. Regarding water pressure dissipation before reaching the maximum temperature, Gens et al. [11] observed a similar response under in-situ conditions, in which pore pressure evolutions did not match the temperature. Numerical analyses of these heating/cooling tests under different hydraulic boundary conditions are

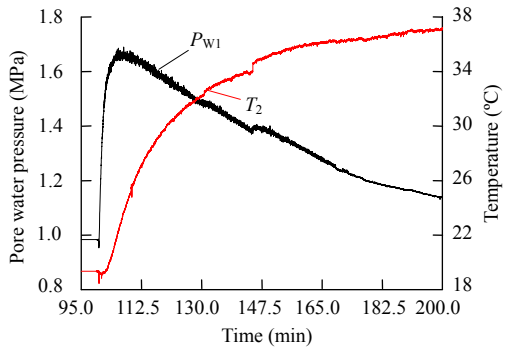

(a) Heating phase.

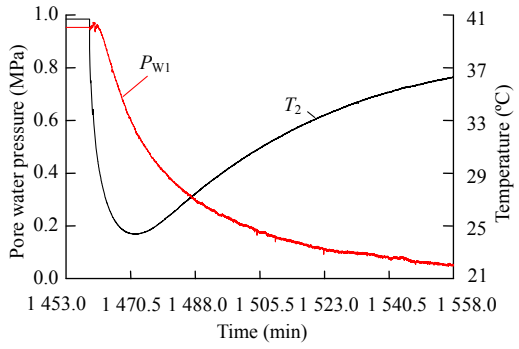

(b) Cooling phase.

Fig.7 Zoom of time evolution of pore water pressure (P_{w1}) and temperature (T_2) changes during thermal stage 4.

currently being performed to explain these observed features.

4 Conclusions

A series of tests along heating and cooling paths were performed on Boom clay, a potential host formation for geological disposal of high-level nuclear waste in Belgium, to study the impact and consequences of thermal loading on this deep clay formation. Thermal tests were performed in a fully-instrumented heating cell with several thermocouples and pressure transducers under nearly constant volume and controlled hydraulic boundary conditions. Selected results of a comprehensive experimental programme on intact borehole samples retrieved in the horizontal direction were presented and discussed in terms of the joint measurements of temperature and pressure changes during the application of heating/cooling cycles. A value of the quasi-undrained pressurisation coefficient, defined as the pore pressure increase due to unit temperature increase, about 0.013 MPa/^{o}C, was obtained when plotting water pressure changes in different quasi-undrained heating/cooling stages at maximum and minimum temperatures. When comparing simultaneously the time evolutions of pressures and temperatures, it was observed that water pressure changes developed at a faster velocity compared with temperature changes during the quasi-undrained heating and cooling consitions. In addition, pore water pressures started to dissipate or increase towards the hydraulic boundary condition applied before the temperature reached its maximum or minimum value in the heating or cooling phase, i.e. pore pressure evolution did not match the temperature one.

The extensive data collected are currently being used to calibrate thermal and hydraulic properties by gathering thermal, hydraulic and mechanical results using a fully coupled thermo-hydro-mechanical code.

Acknowledgements

The authors acknowledge the financial support provided by EIG EURIDICE/SCK•CEN (Belgium) through a PhD collaboration project with International Centre for Numerical Methods in Engineering (CIMNE, Spain).

References

[1] Sultan N. Etude du comportement thermo-mécanique de l'argile de Boom: expériences et modélisation. PhD Thesis. Paris: CERMES, Ecole Nationale des Ponts et Chaussées, 1997 (in French).

[2] De Bruyn D. Influence of a temperature increase on the physical and mechanical behaviour of the Boom clay in the framework of the HLW geological disposal. PhD Thesis. Louvain-La-Neuve: UCL, 1999 (in French).

[3] Le T T. Comportement thermo-hydro-mécanique de lárgile de Boom. PhD Thesis. Paris: CERMES, Ecole Nationale des Ponts et Chaussées, 2008 (in French).

[4] Muñoz J J, Alonso E E, Lloret A. Thermo-hydraulic characterisation of soft rock by means of heating pulse tests. Geotechnique, 2009, 59 (4): 293–306.

[5] Lima A, Romero E, Pineda J A. Low-strain shear modulus dependence on water content of a natural stiff clay. In: XIV Congresso Brasileiro de Mecânica dos Solos e Engenharia Geotécnica. Búzios: [s.n], 2008: 1–6.

[6] Coll C, Escoffier S, Hamza R W, et al. EC SELFRAC project: state of the art on fracturation and sealing-healing processes and characterisation. Mol: EURIDICE, 2004.

[7] Coll C. Endommagement des roches argileuses et perméabilité induite au voisinage d'ouvrages souterrains. PhD Thesis. Grenoble: Université Joseph Fourier, 2005 (in French).

[8] Horseman S T, Winter M G, Entwistle D C. Geotechnical characterization of Boom clay in relation to the disposal of radioactive waste. [S.l.]: Commission of the European Communities, 1987.

[9] Agar J G, Morgenstern N R, Scott J D. Thermal expansion and pore pressure generation in oil sands. Canadian Geotechnical Journal, 1986, 23 (3): 327–333.

[10] Vaziri H H, Byrne P M. Numerical analysis of soil sand under nonisothermal conditions. Canadian Geotechnical Journal, 1990, 27 (6): 802–812.

[11] Gens A, Vaunat J, Garitte B, et al. In-situ behaviour of a stiff layered clay subject to thermal loading observations and interpretation. Geotechnique, 2007, 57 (2): 207–228.